Investigation of Degradation Effects on Crystallization of Thermoplastic Composites

Mathew Wynn; Navid Zobeiry

CITE THE PUBLISHED RECORD

Wynn, M., and Zobeiry, N. (2023). “Investigation of Degradation Effects on Crystallization of Thermoplastic Composites.” SAMPE 2023, Society for the Advancement of Material and Process Engineering.

DOI: https://doi.org/10.33599/nasampe/s.23.0216

SAMPE publication page

RELATED JOURNAL PUBLICATION

Related prior journal article (distinct publication): Investigating the Effect of Temperature History on Crystal Morphology of Thermoplastic Composites Using In Situ Polarized Light Microscopy and Probabilistic Machine Learning, Polymers 15(1) (2023), 18, https://doi.org/10.3390/polym15010018

INVESTIGATION OF DEGRADATION EFFECTS ON CRYSTALLIZATION OF THERMOPLASTIC COMPOSITES

Mathew Wynn[1], Navid Zobeiry[1]
1- Materials Science & Engineering Department, University of Washington
Seattle, WA

ABSTRACT

Thermoplastic composites such as PEKK or PEEK reinforced with carbon fibers go through heating and consolidation steps during processing. Upon heating and subsequent cooldown, a semi-crystalline structure nucleates and grows in the molten polymer. However, thermal degradation or partial oxidation of thermoplastics may severely affect this process and impact their mechanical properties as well as chemical resistance to common solvents. This also affects the recyclability of the material, as well as available repair-time or time to bring large-scale parts to melt. This paper presents a novel approach to investigate and quantify degradation effects in thermoplastic composites using a combination of polarizing light microscopy (PLM), Fourier transform infrared (FTIR) spectroscopy, and machine learning (ML) analysis. While PLM is used for in-situ investigation of the effect of degradation on crystallization, FTIR and ML are used for in-vitro analysis of degradation effects on chemical signature of the material. The results can be used to potentially develop robust manufacturing processes to optimize performance while minimizing degradation.

Keywords: Degradation, Machine Learning, FTIR

Corresponding author: Navid Zobeiry

1. INTRODUCTION

The potential use of thermoplastic composites in the aerospace industry has been studied for many years, but their use has been limited due to manufacturing issues as well as poor resistance to fluids commonly used in aircraft operations, such as hydraulic fluid, fuel, and deicing fluid. However, some thermoplastic matrices, such as polyetheretherketone (PEEK) and polyetherketoneketone (PEKK), which have similar mechanical properties to structural thermoset composites and sufficient chemical resistance, have found some success. For example, PEEK composites have been used in overmolded aerospace brackets and in the mechanical arm of the International Space Station [1], [2]. These types of thermoplastic composite parts are often consolidated using manufacturing techniques like automated tape placement, compression molding, or autoclave consolidation and can be welded together using techniques such as induction welding or resistance welding [3], [4]. Crystallization mainly occurs on cooldown from melt. The crystallinity of the material, which is influenced by processing variables such as fiber volume fraction, dwell time and temperature, and melt history, directly affects the mechanical properties and chemical resistance of the finished part.

Semi-crystalline thermoplastics, like PEEK and PEKK, form crystal structures called spherulites which are made up of folded polymer chains called lamellae, and form when they cool from the molten state. These spherulites can be observed using transmission polarizing light microscopy (PLM). The presence of a fiber reinforcement can create another crystal structure called transcrystallinity, in which the lamellae radiate from the surface of the fiber. These materials also contain self-nuclei, which serve as nucleation sites for the formation of spherulites during cooling and can survive at temperatures above the melting point of the material. The presence of self-nuclei leads to increased nucleation of spherulites, which will likely decrease the size of the resulting spherulites. Kumar et al. observed that self-nuclei remain up to 420 °C, while Jonas and Legras observed self-nuclei no longer remained after a short time at 400 °C [5], [6].

Semi-crystalline thermoplastics, such as PEEK and PEKK, will degrade if they are held at or above their melting temperature for an extended period of time. This degradation is worsened by higher melt temperatures and the presence of oxygen. Degraded material has a higher glass transition temperature (Tg), lower crystallinity, and lower melting temperature [7]. These changes likely occur due to random molecular scission and subsequent cross-linking [8]. Specifically, bonds can occur within the polymer chain or between chains [9]. These changes to the polymer reduce recyclability and reworkability as well as alter its mechanical and thermal properties.

Changes in the polymer due to degradation can be detected using Fourier transform infrared (FTIR) spectroscopy for both PEEK and PEKK. Typically, FTIR analysis such as this will be performed qualitatively by observing changes from a baseline spectrum. The use of machine learning techniques in composites has become more common in recent years [10]–[14]. Methods such as Gaussian Process Regression (GPR) or Principal Components Analysis (PCA) provide a quantitative method for detecting changes in FTIR spectra [15]. These methods are commonly used in other fields like chemometrics. For example, PCA was used to identify archaeological ceramics in FTIR and GPR to interpolate in near infrared [16], [17].

In this study, we present a method for quantifying the extent of degradation in semi-crystalline thermoplastic composites using PCA and GPR on FTIR data. We also demonstrate the effect of degradation on crystal growth in PEEK film using in situ PLM. This method allows for the repeatable detection of degradation in these materials. We applied this approach to PEEK film and PEKK carbon fiber prepreg that was processed multiple times at different melt temperatures in a hot stage, and also evaluated the effect of oxygen versus an inert nitrogen atmosphere on degradation.

2. EXPERIMENTATION

The polymer film used in this study is 25 µm thick from Victrex (2000 series Aptiv), and the prepreg is PEKK-FC/AS4D from Solvay. Squares of approximately 0.25 by 0.25 inches in size were cut from the material. One sample was placed directly onto a microscopic glass slide, and four other samples were placed onto a piece of Kapton film surrounding the first sample. The glass slide, Kapton film, and samples were placed onto the heating block in a Linkam THMS600 hot stage, as shown in Figure 1. The sample placed directly onto the glass provides a representative view of the all the samples and allows for in situ polarizing light microscopic (PLM) observation of crystal growth [10], [18]. However, this sample cannot be removed because it becomes bonded to the glass. The samples placed onto the Kapton film can be removed and further analyzed.

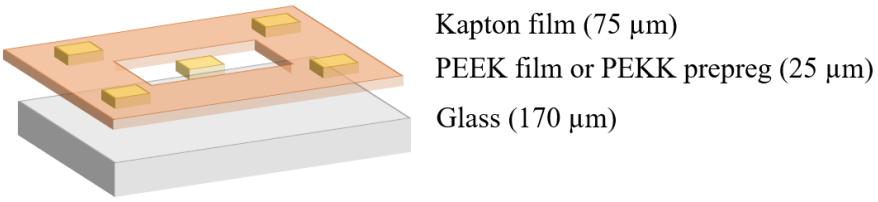

Figure 1. Sample configuration used in THMS600 hot stage.

Samples were heated in the THMS600 hot stage in both air and nitrogen. The samples were heated at a rate of 20 °C/min to 120 °C and held for 10 minutes to remove moisture, then heated to the melt temperature at a rate of 20 °C/min and held for 10 minutes. Three melt temperatures were used for each material. The PEEK film used 385 °C as a standard melt temperature, 420 °C as an extreme high, and 400 °C as a midpoint. The temperature of 420 °C is significant as it should ensure the removal of prior crystallization [5], [6]. For PEKK, which has a lower melting temperature, the temperatures of 410 °C, 392.5 °C, and 375 °C were used. After melting, the samples were cooled down at a rate of 140 °C/min to 285C for PEEK and 275 °C for PEKK, and held for 10 minutes. The samples were then cooled down to 143 °C (T_g) at a rate of 65 °C/min. The cooldowns were as fast as possible using the THMS600 without active cooling to minimize crystallization during cooldown. The heating cycles are shown in Figure 2.

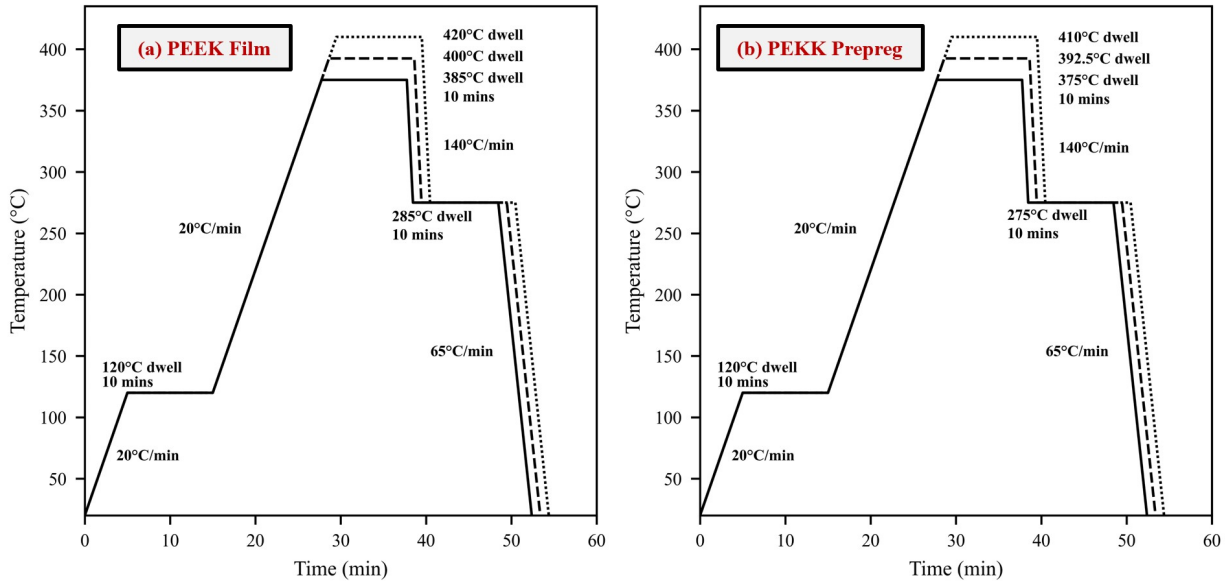

Figure 2. THMS600 heating cycles showing dwells and heating rates. (a) shows the heating cycle for PEEK film (b) shows the heating cycle for PEKK prepreg.

The center sample, as shown in Figure 1, was observed under an Olympus BX61 polarizing light microscope. Video was recorded during heating, melting, and crystallization.
Samples were processed three times at each melt temperature. After each heating cycle, FTIR spectroscopy was performed on the samples using a Bruker Vertex 70 with an attenuated total reflection (ATR) accessory, PIKE GladiATR. The samples were measured from 1900cm^{-1} to

400cm^{-1} with a spectral resolution of 1 cm^{-1}, using 64 scans before Fourier transform. Two example FTIR spectra are provided in Figure 3, in which process extremes are compared to illustrate the difference after thermal degradation. The spectra intensities have been normalized.

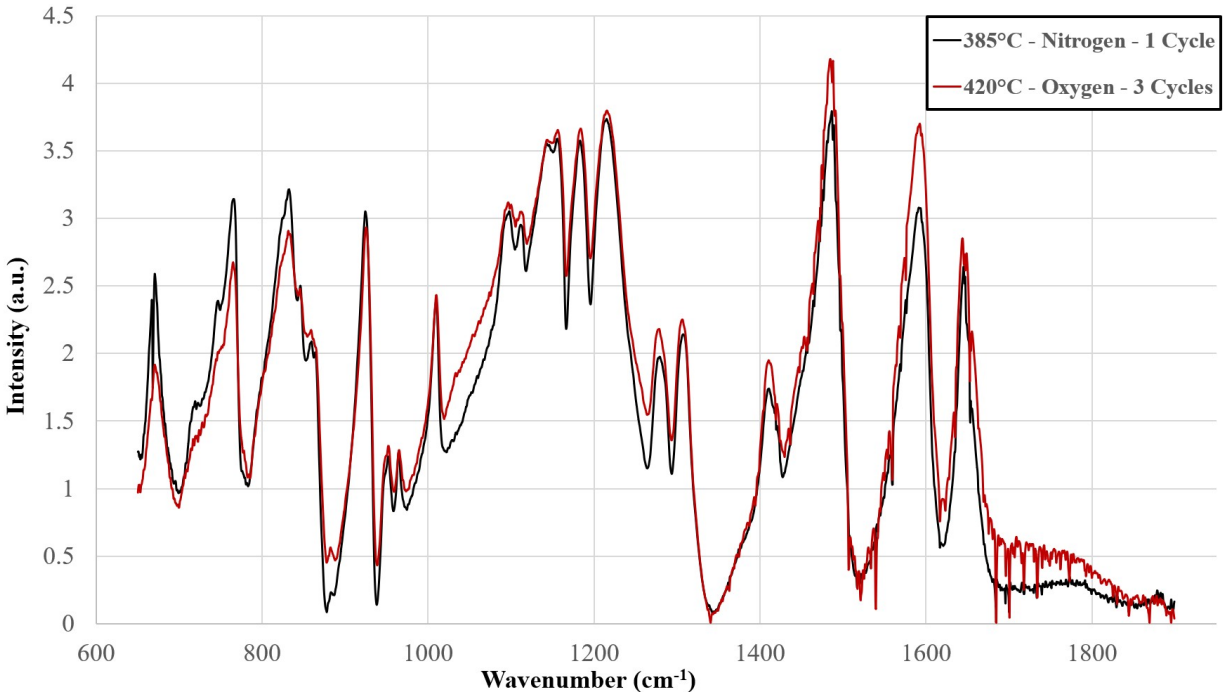

Figure 3. FTIR spectra comparison for PEEK film treated at 385 °C in nitrogen and one cycle, and 420 °C in oxygen and three cycles.

Principal components analysis (PCA) was used for dimensionality reduction, grouping of samples by principal components, and identification of the peaks that contributed most to variance. Gaussian process regression (GPR) was used to train a model to correlate process parameters and principal components identified by PCA. The Scikit-learn library in Python was used for both PCA and GPR.

3. RESULTS AND DISCUSSION

3.1 Polarized Light Microscopy

PLM is a through transmission technique, which means that light is blocked by carbon fibers. As a result, the PEKK prepreg samples could not be observed using PLM. For most of the PEEK film samples, the growth rate was too fast to be reliably captured in video. End-state example micrographs are presented in Figure 3 for 420 °C in nitrogen. After one cycle as shown in Figure 3(a), spherulites are 20-30 µm in diameter. Figure 3(b) shows that the crystals are about double the size at 45-60 µm after another 420 °C cycle. One more cycle in Figure 3(c) shows a few small crystals at 4-8 µm surrounded by amorphous material. In general, repeated cycles and higher melt temperatures leads to larger crystals. As the polymer degrades, less material is available for nucleation which lowers the nucleation rate. A lower nucleation rate will create larger crystals as the crystals that do nucleate will have more room to grow before impingement [6]. In the case of

Figure 3(c), growth was slow enough that after 10 minutes impingement had not occurred, and upon cooldown the rest of the molten polymer was left amorphous. Given enough time, the sample in Figure 3(c) would have likely created spherulites larger than those in Figure 3(b).

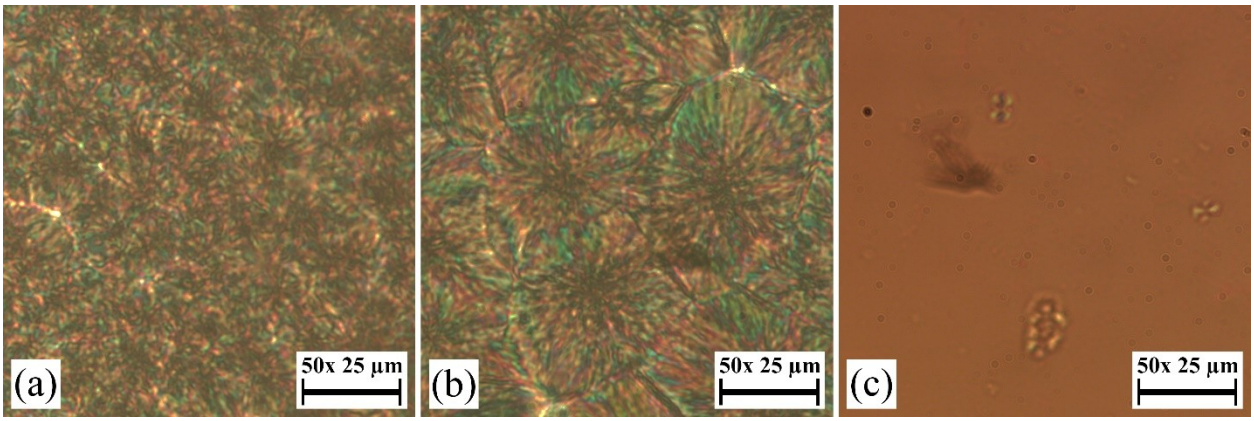

Figure 4. Micrographs of a PEEK film after thermal cycling at 420 **°C** in nitrogen. (a) shows 20-30 µm spherulites after one cycle (b) two cycles yields 45-60 µm crystals (c) three cycles leads to incomplete growth and 4-8 µm spherulites.

3.2 Principal Components Analysis

PCA was performed on the FTIR spectra data to reduce the data to four principal components. Only 1900cm^{-1} to 650cm^{-1} was evaluated as the 650cm-1 to 400cm-1 range is noisy and does not contribute to identifying functional groups involved in degradation. Data was normalized before PCA. The first four principal components explained 90.1 % of the variance for the combined dataset. The first and second principal components are plotted in a score plot for both materials as shown in Figure 4. Two sets of clear groupings can be identified between the PEEK film and PEKK prepreg. This likely is due to differences in the polymer chains as well as the presence of carbon fiber in the PEKK prepreg.

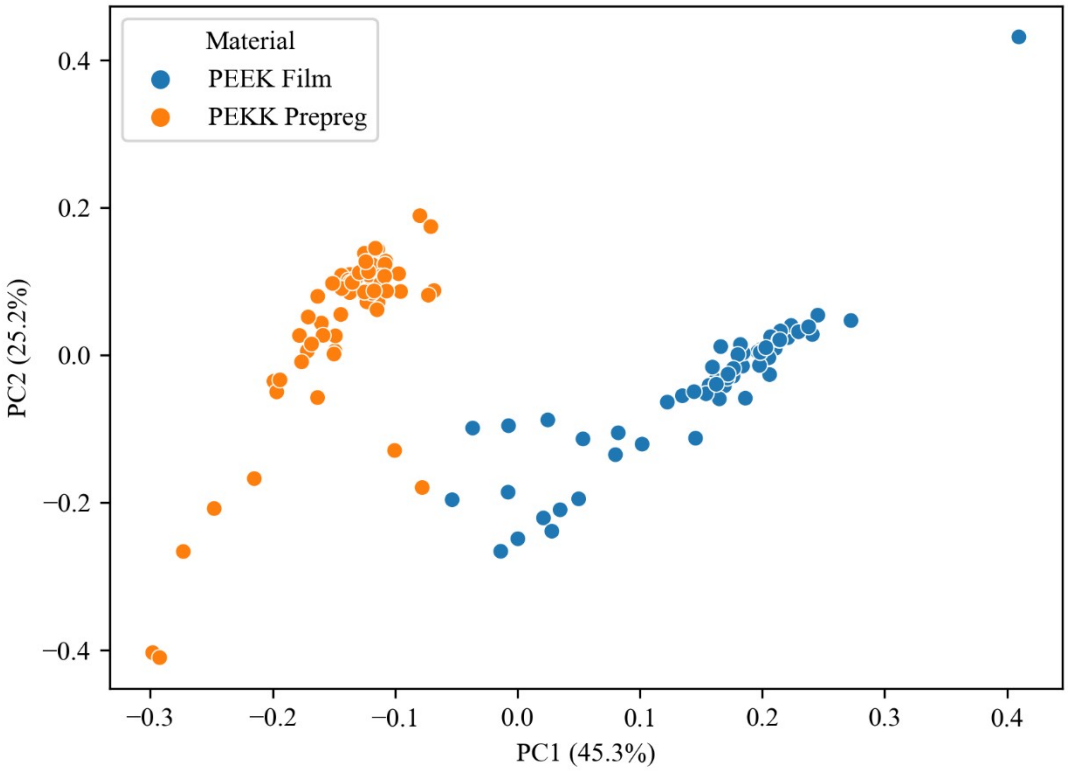

Figure 5. Score plot showing both the PEEK film and PEKK prepreg indicating a significant difference between the materials.

As the materials are in clearly segregated groups and the differences can be explained without involving degradation, PCA was repeated for each material on its own. Table 1 shows the contributions to variance for the first four components for each material. PEKK has a much higher contribution from the first component, whereas the first three components in PEEK contribute significantly.

Table 1. Variance explained by principal components for PEEK film and PEKK prepreg.

Material	PC1 (%)	PC2 (%)	PC3 (%)	PC4 (%)
PEEK Film	42.3	31	15.6	3.8
PEKK Prepreg	67.3	13.3	5.5	3.2

Score plots between the first two components were generated for both PEEK and PEKK. Melt temperatures, cycles, and environment were compared. Some clustering might exist for the 400 °C melt temperature in PEEK, but besides that, no obvious clustering was identified.

The normalized FTIR spectra were input into the Origin software package and a 2nd derivative was calculated for all data. This was done to identify the peaks that contributed most to variance [16]. PCA was performed on these 2nd derivative values, and the peaks associated with the principal components were identified. Peaks that had loading values greater than 0.05 are identified in Table 2. The functional groups identified are similar to those that have been found in previous thermal degradation work on PEEK [9]. Peaks in the 1700cm^{-1} to 1733cm^{-1} range that contributed to variance are likely due to intramolecular bonding and the formation of dibenzocyclopentanones. At 1684cm^{-1} and 1650cm^{-1}, peaks are attributed to ketone stretching near the benzenes. 1635cm^{-1} is likely due to C=C stretching at the benzophenone, and 667cm^{-1} and 668cm^{-1} due to C=C bending. Changes in these FTIR peaks are attributed to degradation involving intramolecular bonding [9]. Intermolecular bonding and cross-linking were notably not identified. When Pascual et al. identified these peaks, the PEEK sample was exposed to considerably more thermal energy and the sample was near char [9]. Cross-linking may not be detectable in FTIR in PEEK except in extreme thermal exposures.

Table 2. Wavenumbers and functional groups identified by PCA.

Wavenumber (cm^{-1})	Functional Group
1700-1733	Formation of dibenzocyclopentanones
1684, 1650	Ketone stretching around benzenes
1635	C=C stretching at benzophenone
667-668	C=C stretching, bending

3.3 Gaussian Process Regression

For GPR training, a covariance matrix (kernel) is selected. The kernel is incorporated by GPR to make predictions and provides uncertainty measures over those predictions. During training, the posterior distribution is updated as data is introduced, reducing uncertainty and improving predictions [19].

Data was split into 80 % training data and 20 % validation data. The hyperparameter n_restarts_optimizer was set to 20. The dot-product kernel was cubed and combined with the radial basis function and white noise kernel:

$$\Sigma\left(x_i, x_j\right) = c * \left[\sigma_0^2 + x_i \bullet x_j\right]^3 + c * \exp\left(-\frac{d\left(x_i, x_j\right)^2}{2l^2}\right) + \sigma_e^2 I_n \qquad [1]$$

where c is a constant, σ_0^2 is the inhomogeneity of the kernel, $d(x_i,x_j)$ is the Euclidean distance, l is the length scale of the kernel, σ_e^2 is the variance of noise, and I_n is the identity matrix. The length scale l was set to 1, and the default value of unity was used for both σ_0^2 and σ_e^2.

GPR was first performed on the normalized FTIR spectra, but the fit was poor. An additional fit was done on the principal components previously identified. The melt temperature, cycle count, and environment were input variables, and the principal components were response variables. GPR was performed on the PEEK film and PEKK prepreg separately after outliers were removed. In this way, the PEEK film GPR model showed a 59.9 % accuracy, and the PEKK prepreg 35.0 % accuracy. These accuracies are low but indicate there is prediction power by using principal components from FTIR data to detect degradation. One benefit to GPR is it identifies where uncertainty is high, and future work can improve these models with additional testing to fill in the gaps.

The dataset was further separated by environment, and surfaces generated based on GPR fit to see the effect of cycles and melt temperature on the first principal component. In these surfaces, the principal component on the z-axis represents the amount of variation in the underlying FTIR spectra. The GPR surfaces are shown in Figure 6. In Figure 6(a) PEEK film is treated in nitrogen, and PC1 decreases as melt temperature increases and variation is fairly constant between cycles. Figure 6(b) is PEEK in oxygen and has a ridge starting at one cycle and 385 °C melt temperature and diagonally crosses to three cycles and 420 °C melt temperature. When Figure 6(a) and (b) are compared, oxygen induces additional variation particularly across cycles. Figure 6(c) is PEKK prepreg treated in nitrogen and is fairly flat across cycles and melt temperatures. PEKK in oxygen as shown in Figure 6(d) is similar and has little change across cycles or melt temperature. Comparing PEEK film in Figure 6(a) and (b) with PEKK prepreg in (c) and (d), the fibers and lower volume of polymer likely diminish the variation that can be detected in FTIR.

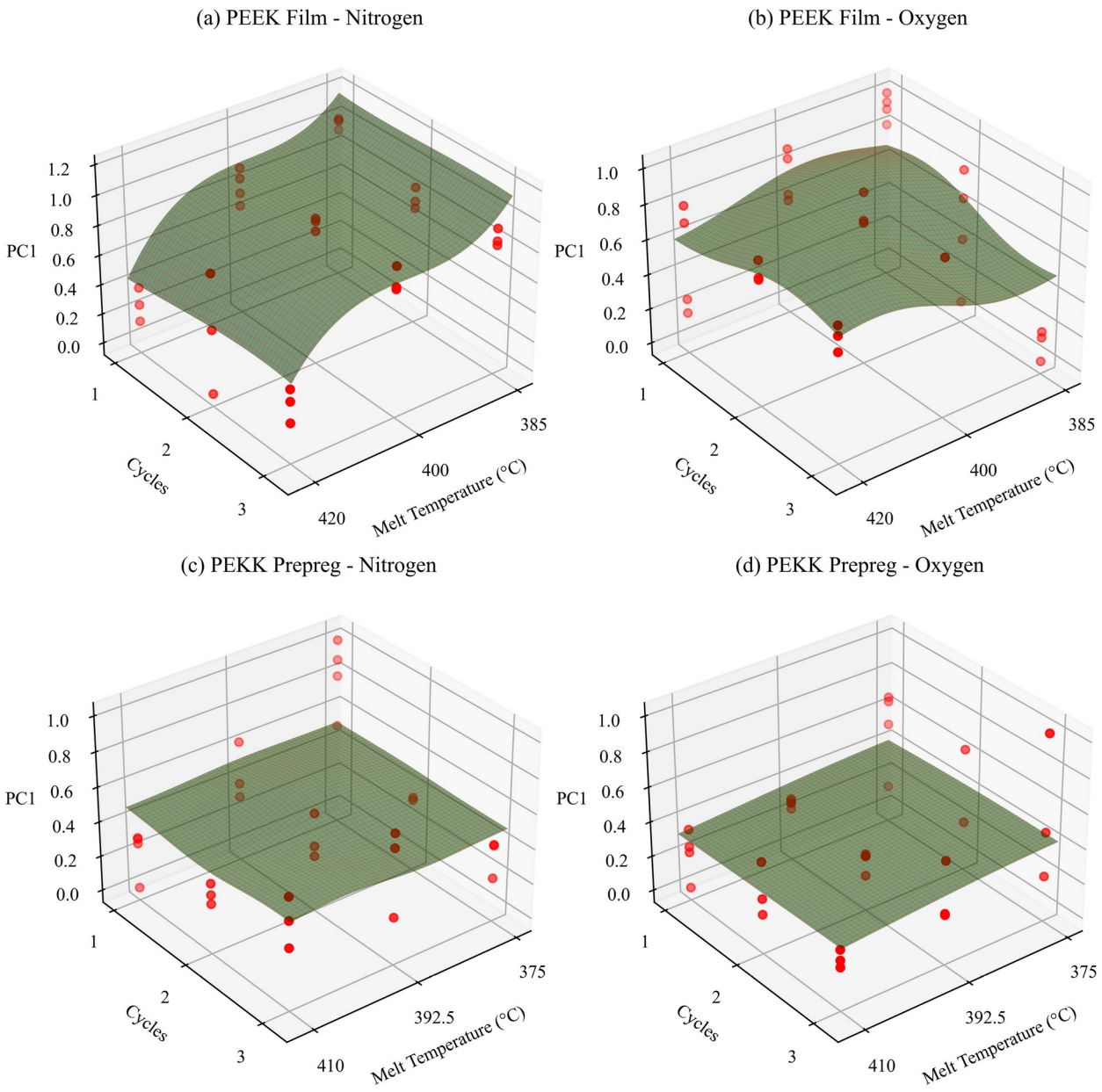

Figure 6. GPR surfaces fit for cycle count, melt temperature, and PC1 (a) shows PEEK film in nitrogen and varies with melt temperature (b) illustrates PEEK film with oxygen and varies in both cycles and melt temperature (c) shows PEKK prepreg in nitrogen and has little variation (d) illustrates PEKK prepreg with oxygen and also has little variation.

4. CONCLUSIONS

This study provided a proof-of-concept GPR model based on principal components. With further work, this model could be used to identify thermal degradation that can result from processing thermoplastic composite parts. The model could potentially be used to develop robust manufacturing processes that optimize performance while minimizing degradation.

- PLM showed that nucleation was significantly reduced during repeated cycling, especially at high melting temperatures. This thermal exposure clearly affects subsequent crystal formation, which is likely due to degradation of the polymer matrix.

- PCA was shown to successfully identify variation in FTIR when materials were compared. The differences between materials are likely due to the presence of carbon fiber in the PEKK prepreg, and the difference in monomer between PEEK and PEKK. These differences cannot be attributed to degradation.

- Comparing the effects of melt temperature, cycle count, and environment using PCA score plots showed no obvious clustering, except perhaps in the PEEK film when melted at 400 °C.

- The principal components identified by PCA were related to functional groups involved in intramolecular bonding. No functional groups involved in intermolecular bonding or cross-linking were identified.

- GPR trained on principal components identified from PCA performed on FTIR spectra attained 46 % accuracy for PEEK film and 30 % accuracy for PEKK prepreg. These accuracies are low, but are a proof-of-concept for this method. Future work can collect data strategically identified to reduce uncertainty identified by the GPR model.

- GPR surfaces were fit for cycle count, melt temperature, and PC1 based on data separated by material and environment. Accuracies were low except for PEEK film in oxygen which had a 61 % accuracy. In this case, the surface trended as expected with expected degradation.

ACKNOWLEDGMENTS

We would like to acknowledge financial support by the University of Washington and the State of Washington in the USA, as well as in-kind contributions of Victrex plc and Daher.

5. REFERENCES

[1] S. Green, F. J. Ferfecki, and U. Marburger, “Overmoulding of PEEK Compounds for Composites Aerospace Brackets,” *S.A.M.P.E. J.*, vol. 54, no. 3, pp. 22–29, 2018.

[2] J. Denault and M. Dumouchel, “Consolidation Process of PEEK/Carbon Composite for Aerospace Applications,” *Adv. Perform. Mater.*, vol. 5, pp. 83–96, 1998.

[3] L. Ye, K. Friedrich, J. Kästel, and Y.-W. Mai, “Consolidation of unidirectional CF/PEEK composites from commingled yarn prepreg,” *Compos. Sci. Technol.*, vol. 54, no. 4, pp. 349–358, Jan. 1995, doi: 10.1016/0266-3538(95)00061-5.

[4] M. Dubé, P. Hubert, A. Yousefpour, and J. Denault, “Resistance welding of thermoplastic composites skin/stringer joints,” *Compos. Part A Appl. Sci. Manuf.*, vol. 38, no. 12, pp. 2541–2552, Dec. 2007, doi: 10.1016/j.compositesa.2007.07.014.

[5] S. Kumar, D. P. Anderson, and W. W. Adams, “Crystallization and morphology of poly(aryl-ether-ether-ketone),” *Polymer (Guildf).*, vol. 27, no. 3, pp. 329–336, 1986, doi: 10.1016/0032-3861(86)90145-X.

[6] A. Jonas and R. Legras, “Thermal stability and crystallization of poly(aryl ether ether ketone),” *Polymer (Guildf).*, vol. 32, no. 15, pp. 2691–2706, 1991, doi: 10.1016/0032-3861(91)90095-Z.

[7] P. Tsotra, M. Toma, A. Pascual, F. Schadt, C. Brauner, and C. Dransfeld, “Thermo-Oxidative Degradation of Peek At High Temperatures,” *ECCM18 – 18th European Conference on Composite Materials* Athens, Greece, Jun 24-28 2018, pp. 24–28.

[8] M. Day, D. Sally, and D. M. Wiles, “Thermal degradation of poly(aryl-ether-ether-ketone): Experimental evaluation of crosslinking reactions,” *J. Appl. Polym. Sci.*, vol. 40, no. 910, pp. 1615–1625, Nov. 1990, doi: 10.1002/app.1990.070400917.

[9] A. Pascual, M. Toma, P. Tsotra, and M. C. Grob, “On the stability of PEEK for short processing cycles at high temperatures and oxygen-containing atmosphere,” *Polym. Degrad. Stab.*, vol. 165, pp. 161–169, 2019, doi: 10.1016/j.polymdegradstab.2019.04.025.

[10] M. Wynn and N. Zobeiry, “Investigating the Effect of Temperature History on Crystal Morphology of Thermoplastic Composites Using In Situ Polarized Light Microscopy and Probabilistic Machine Learning,” *Polymers (Basel).*, vol. 15, no. 1, p. 18, Dec. 2022, doi: 10.3390/polym15010018.

[11] Y. Freed, M. Salviato, and N. Zobeiry, “Implementation of a probabilistic machine learning strategy for failure predictions of adhesively bonded joints using cohesive zone modeling,” *Int. J. Adhes. Adhes.*, vol. 103226, 2022.

[12] N. Zobeiry and K. D. Humfeld, “A physics-informed machine learning approach for solving heat transfer equation in advanced manufacturing and engineering applications,” *Eng. Appl. Artif. Intell.*, vol. 101, p. 104232, May 2021, doi: 10.1016/j.engappai.2021.104232.

[13] K. Manohar, T. Hogan, J. Buttrick, A. G. Banerjee, J. N. Kutz, and S. L. Brunton, “Predicting shim gaps in aircraft assembly with machine learning and sparse sensing,” *J. Manuf. Syst.*, vol. 48, pp. 87–95, Jul. 2018, doi: 10.1016/j.jmsy.2018.01.011.

[14] C. Sacco, A. Baz Radwan, A. Anderson, R. Harik, and E. Gregory, “Machine learning in composites manufacturing: A case study of Automated Fiber Placement inspection,” *Compos. Struct.*, vol. 250, p. 112514, Oct. 2020, doi: 10.1016/j.compstruct.2020.112514.

[15] C. Schoenholz *et al.*, “A MACHINE LEARNING-BASED PORTABLE INSPECTION METHOD FOR EVALUATION OF TOOL SURFACE CONDITION AND RELEASE COATING IN COMPOSITES MANUFACTURING,” *SAMPE Conference Proceedings* Charlotte, North Carolina, May 23-26, 2022. Society for the Advancement of Material and Process Engineering. doi: 10.33599/nasampe/s.22.0740

[16] L. Medeghini, S. Mignardi, C. De Vito, and A. M. Conte, “Evaluation of a FTIR data pretreatment method for Principal Component Analysis applied to archaeological ceramics,” *Microchem. J.*, vol. 125, pp. 224–229, 2016, doi: 10.1016/j.microc.2015.11.033.

[17] D. Leamy, T. Ward, and J. Kocijan, “Using Gaussian Process Models for Near-Infrared Spectroscopy Data Interpolation,” *Proceedings of the 7th IASTED International Conference* Innsbruck, Austria, Feb 17-19, 2010, doi: 10.2316/J.2010.216.680-0160.

[18] M. Wynn and N. Zobeiry, “A Fast Method for Evaluating Effects of Process Parameters on Morphology of Semi-Crystalline Thermoplastic Composites,” *Proceedings of the American Society for Composites – 36th Technical Conference on Composite Materials.* Virtual, September 19-23, 2021.

[19] J. Wang, “An Intuitive Tutorial to Gaussian Processes Regression,” Sep. 2020, Available: http://arxiv.org/abs/2009.10862.